

Supporting Information

A Cluster-Based Mesoporous Ti-MOF with Sodalite Supercages

Table of Contents

| | |
|--|---|
| 1. Experimental details..... | 3 |
| 2. Synthesis of the MTM-1 | 3 |
| 3. Crystallographic details | 3 |
| 4. Structure of the MTM-1 | 4 |
| 5. Powder X-ray diffraction | 6 |
| 6. The pore size distribution curve..... | 6 |
| 7. FT-IR spectrum..... | 7 |
| 8. TG-Measurement | 7 |
| 9. Fluorescence spectrum..... | 8 |
| 10. EDX analysis | 8 |
| 11. Photo-degradation..... | 9 |
| References..... | 9 |

1. Experimental details

General. All chemicals were purchased commercially and used without further purification. X-ray powder diffraction (XRD) data were collected on a D8 ADVANCE (Bruker) diffractometer at 40 kV and 30 mA with monochromated Cu K α radiation ($\lambda = 1.5405 \text{ \AA}$) with a scan speed of $5^\circ/\text{min}$ and a step size of 0.02° in 2θ . Elemental analyses for C, H, and N were performed by a VarioEL analyzer. Thermal gravimetric analysis (TGA) was conducted under an air atmosphere with a heating rate of $10^\circ\text{C}/\text{min}$ on a SDT 2960 Simultaneous DSC-TGA of TA instruments up to 800°C . The infrared (IR) spectra (diamond) were recorded on a Nicolet 7600 FT-IR spectrometer within the $4000\text{-}500 \text{ cm}^{-1}$ region. Energy Disperse Spectroscopy (EDS) was obtained by using a scanning electron microscope (Hitachi S-4800) equipped with a Bruker AXS XFlash detector 4010.

N₂ absorption. The N₂ absorption measurement was performed on ASAP 2020 and Autosorb MP-1 apparatuses at 77 K. An activated sample was prepared by exchange of the solvent in the as-synthesized MTM-1 with fresh MeCN followed by evacuation at room temperature. About 120 mg solvent exchanged samples of MTM-1 were loaded into the sample basket within the adsorption instrument (ASAP 2020) and then degassed under dynamic vacuum at 120°C for 10 h to obtain the fully desolvated samples.

Photodegradation of methylene blue (MB) with MTM-1: The evaluation of photocatalytic activities of the samples for the visible light photocatalytic degradation of organic dyes was performed at ambient temperature. A 300-W Xenon lamp coupled with a UV cut-off filter ($420 > \text{nm}$) is employed as light source. The procedure was as follows: 10 mg of sample was dispersed into 20 mL of MB aqueous solution ($10^{-4} \text{ mol L}^{-1}$). Prior to irradiation, the mixture was stirred continuously with a magnetic stirring bar for 2 h in the dark to reach the adsorption equilibrium. Then the dispersions are added H₂O₂ (30%, 50 μL). During the degradation, the mixture was stirred continuously. At given time intervals, 2 mL of analytical samples were withdrawn, centrifuged, and then analyzed by the absorption spectra. The degradation efficiency was determined by dividing C/C_0 , where C is the remained MB concentration and C₀ is the starting MB concentration.

Single-crystal structure determinations. Crystallographic data were collected at 150 K on a Bruker Apex II CCD diffractometer with graphite-monochromated Mo K α radiation ($\lambda = 0.71073 \text{ \AA}$). Data processing was accomplished with the SAINT program. The structures were solved by direct methods and refined. Using Olex², the structure was solved with the ShelXS² structure solution program using Direct Methods and refined with the ShelXL³ refinement package using Least Squares minimisation. All non-hydrogen atoms were refined with anisotropic displacement parameters during the final cycles. All hydrogen atoms of the organic molecule were placed by geometrical considerations and were added to the structure factor calculations. CCDC 1562487 contains the supplementary crystallographic data for this paper. These data can be obtained free of charge from The Cambridge Crystallographic Data Centre via www.ccdc.cam.ac.uk/data_request/cif.

2. Synthesis of the MTM-1

Isonicotinic acid (0.066 g, 0.5 mmol), CuI (0.095 g, 0.5 mmol), are added to acetonitrile (5.0 mL) in a 23 mL Teflon-lined stainless-steel autoclave. Then, Ti(OⁱPr)₄ (153 μL , 0.5 mmol) was added. The resultant solution was heated at 100°C for two days. After cooled to room temperature, large dark red crystals were obtained. (yield: $\sim 100 \text{ mg}$, 60 % based on Ti(OⁱPr)₄). The crystals are rinsed with fresh MeCN and preserved under a sealed and dry environment. Anal. Calcd for C₅₄H₆₆N₆O₂₄Ti₆Cu₃I₃: C, 31.7; H, 2.7; N, 4.1. Found: C, 26.2; H, 2.9; N, 4.3. FT-IR (cm⁻¹): 2971(w), 1587(m), 1541(s), 1413(s), 1217(w), 1021(s), 1057(m), 997(s), 856(w), 764(w), 728(w), 673(s), 614(m).

3. Crystallographic details

Table S1. X-ray measurements and structure solution of compound MTM-1.

| Compound | MTM-1 |
|----------|-------|
|----------|-------|

| | |
|---|---|
| Empirical formula | C ₅₄ H ₆₆ N ₆ O ₂₄ Ti ₆ Cu ₃ I ₃ |
| Formula weight | 2041.6813 |
| Crystal system | cubic |
| Space group | Im-3m |
| a / Å | 32.330(4) |
| V | 33794(7) |
| Z | 4 |
| ρ _{calc} / g·cm ⁻³ | 0.696 |
| μ(MoKα) / mm ⁻¹ | 1.212 |
| F(000) | 6720.0 |
| 2θ range / ° | 1.78-50 |
| Reflections collected/ unique | 2847 / 96606 |
| Data/restraints/ parameters | 2847/0/93 |
| R1/wR ₂ (I > 2σ(I)) ^a | 0.0639 / 0.1780 |
| R1/wR ₂ (all data) | 0.0746 / 0.1868 |
| GooF (all data) ^b | 1.125 |
| Data completeness | 0.991 |
| Max. peak/hole / e ⁻ · Å ⁻³ | 1.29/-0.42 |

$${}^a R_1 = \frac{\sum ||F_o| - |F_c||}{\sum |F_o|}; wR_2 = \left\{ \frac{\sum w[(F_o)^2 - (F_c)^2]^2}{\sum w[(F_o)^2]^2} \right\}^{1/2}$$

$${}^b \text{GooF} = \left\{ \frac{\sum w[(F_o)^2 - (F_c)^2]^2}{(n-p)} \right\}^{1/2}$$

4. Structure of the MTM-1

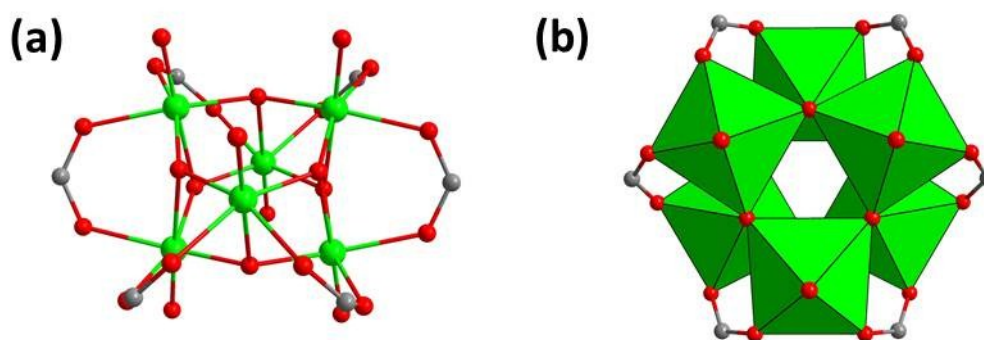


Figure S1. (a) Ball-stick of [Ti₆O₆] core. (b) Structure of the hexagonal cluster.

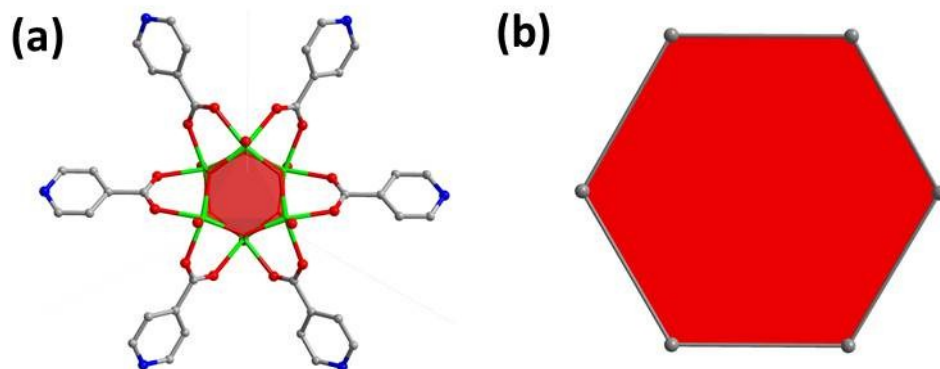


Figure S2. (a) Structure of the hexagonal unit $\{[\text{Ti}_6\text{O}_6][\text{iPrO}]_6[\text{INA}]_6\}$. (b) Six points of extension of the $\{[\text{Ti}_6\text{O}_6][\text{iPrO}]_6[\text{INA}]_6\}$ unit.

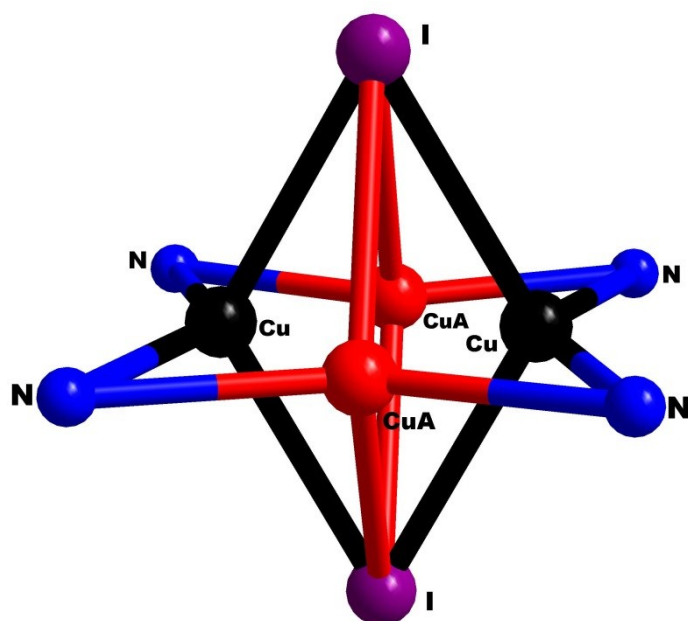


Figure S3. The disorder observed in the Cu_2I_2 dimer. (each occupies its position 50%)

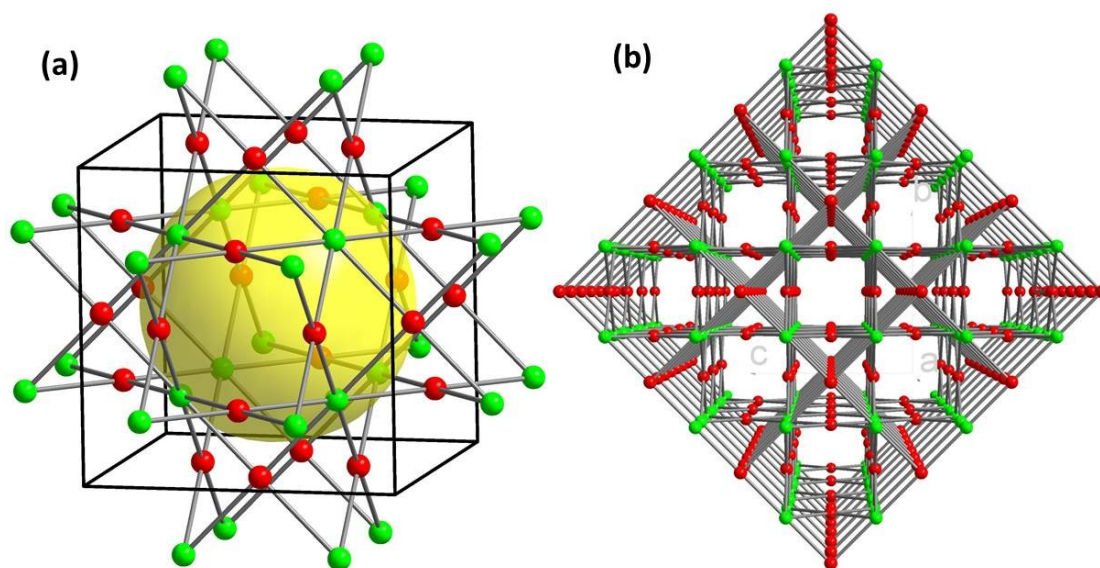


Figure S4. (a) The topology of the cage. The $\{[\text{Ti}_6\text{O}_6][\text{iPrO}]_6\}^{6-}$ cluster simplified as a 6-connecting nodes while the Cu_2I_2 clusters simplified as 4-connecting nodes. (b) 3D topology of MTM-1.

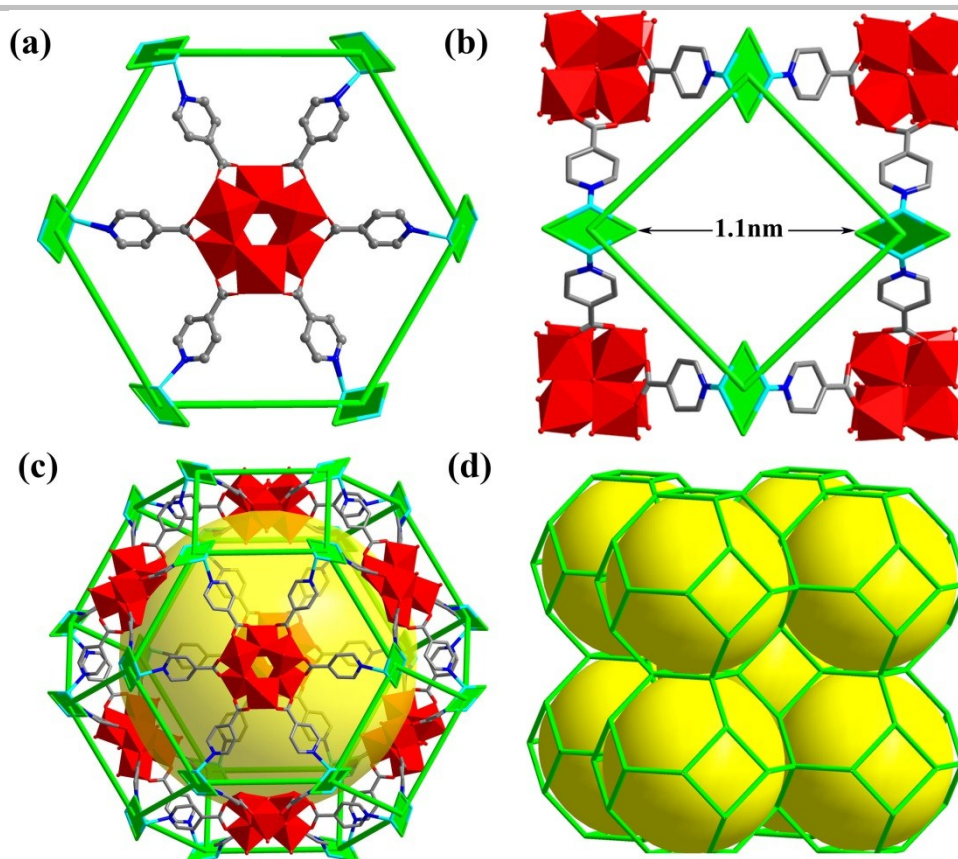


Figure S5. (a) hexagonal planes. (b) Square windows. (c) Topological representation of the cage. (d) The stacking of polyhedral cages in **MTM-1**.

5. Powder X-ray diffraction

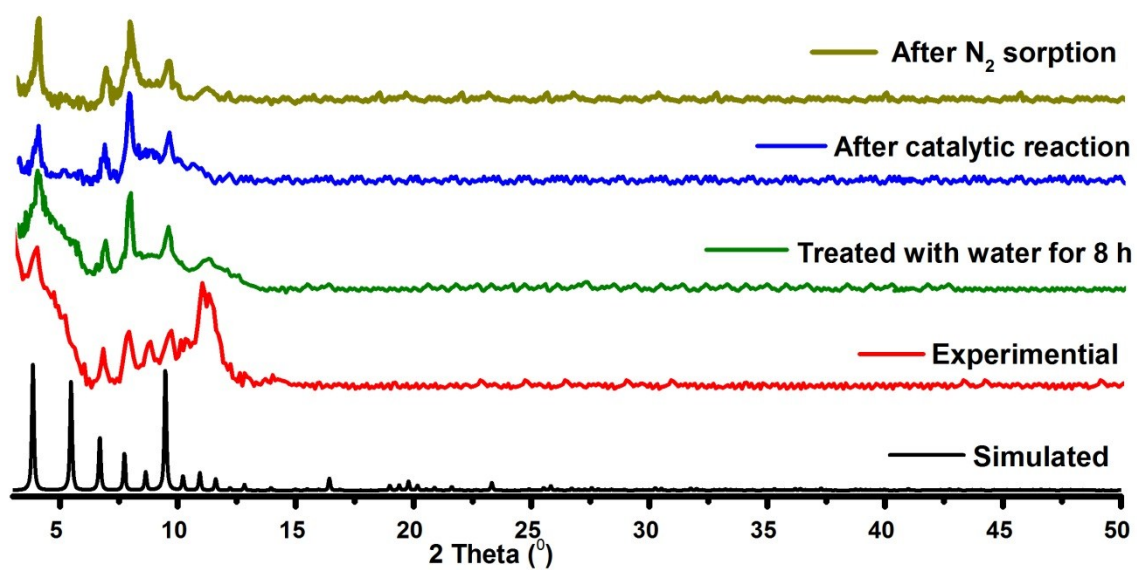


Figure S6. The powder XRD patterns for **MTM-1** under different conditions. The simulated PXRD pattern derived from crystal data after the SQUEEZE process,

6. The pore size distribution curve

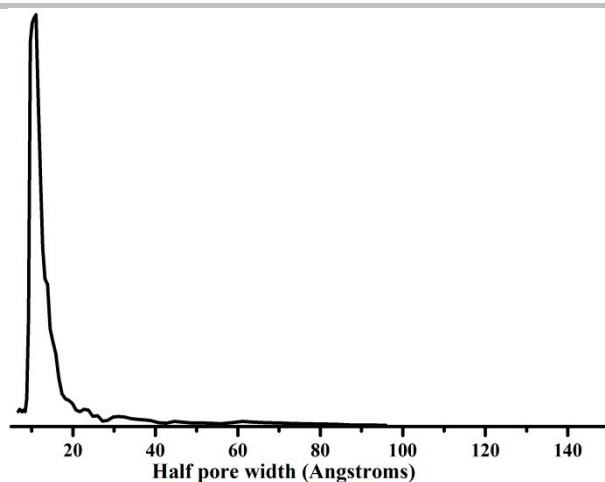
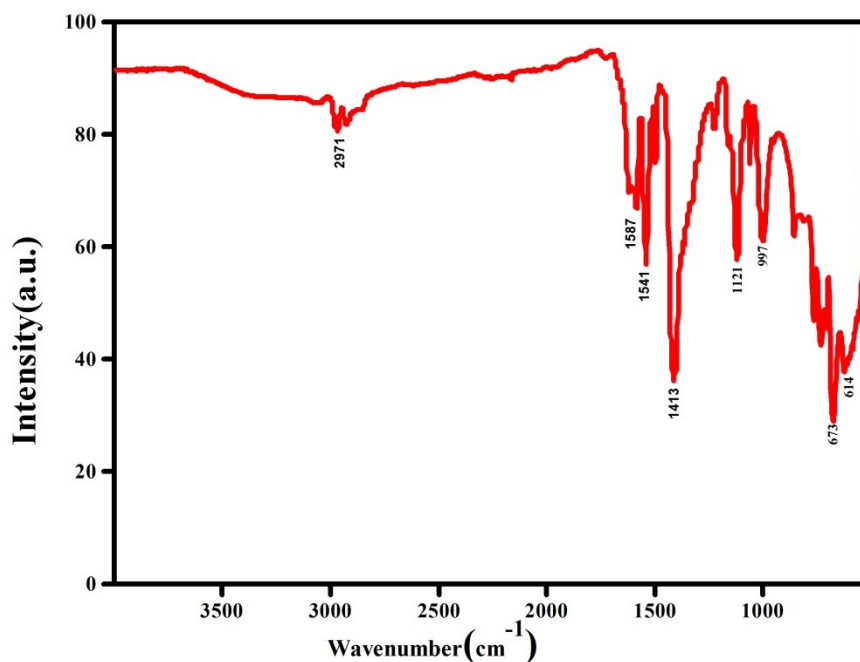


Figure S7. The pore size distribution curve of MTM-1.

7. FT-IR spectrum



Within IR spectrum, the peak around 2971 cm^{-1} is attributed to the phenyl C-H stretching mode. The bands at 1587, 1541, 1500 and 1470 cm^{-1} are assigned to pyridine skeleton vibrational modes. The peaks from the carboxylate ligand were displayed around 1431 cm^{-1} . The strong bands located at 673 and 614 cm^{-1} are dominated by the Ti -O characteristic. The asymmetric and symmetric stretch peaks of ν (Ti-O-C) were observed around 1210 and 997 cm^{-1}

Figure S8. FT-IR spectrum for MTM-1.

8. TG-Measurement

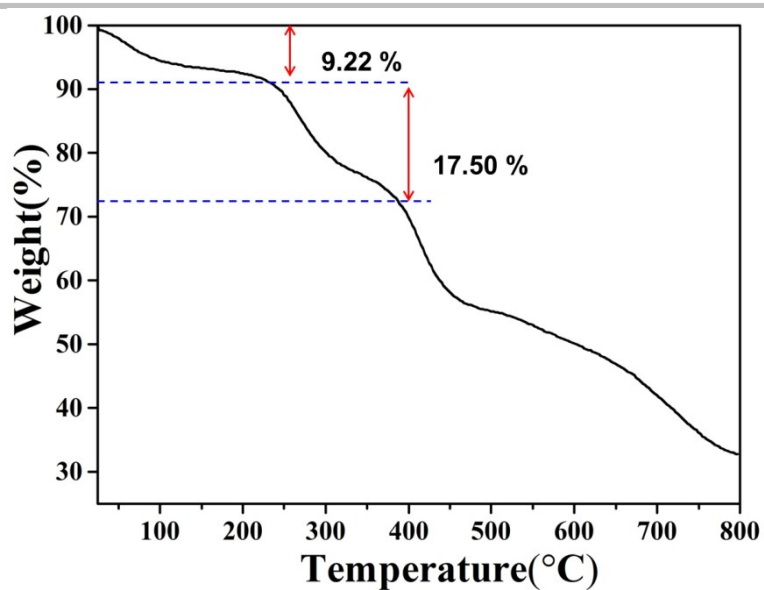


Figure S9. TGA curves of MTM-1.

9. Fluorescence spectrum

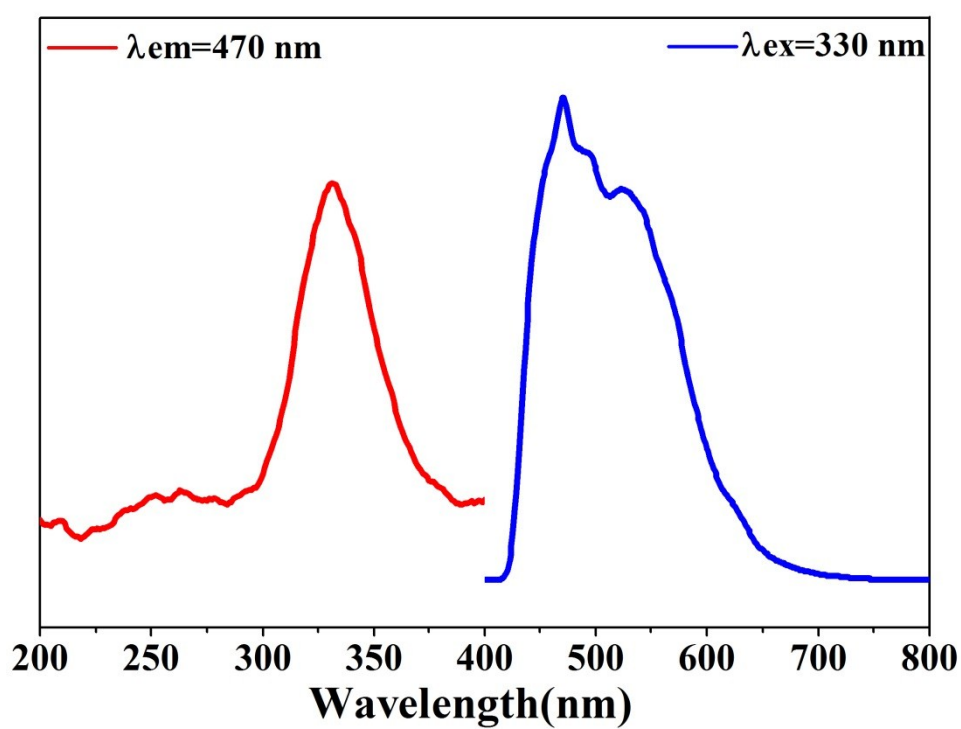
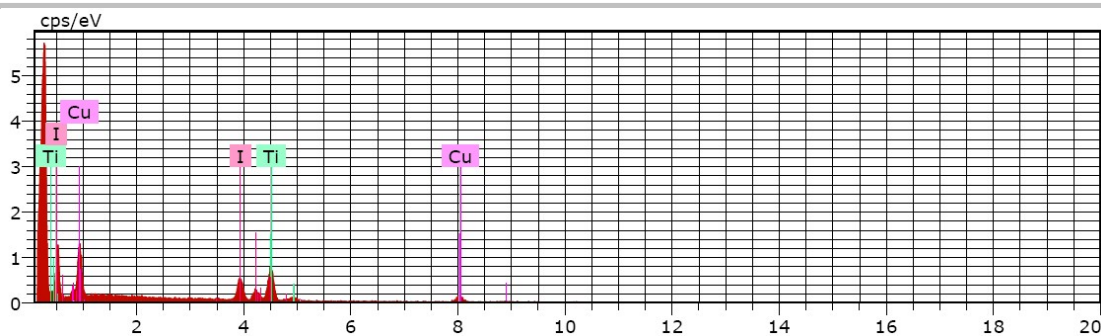


Figure S10. Emission (blue line) and excitation (red line) spectra of MTM-1 in the solid state at room temperature.

10. EDX analysis



The atomic ratio of Ti/Cu/I is 2.1:1.08:1, which is in good agreement with the experimental crystallographic data.

Figure S11. EDX analysis of MTM-1.

11. Photo-degradation

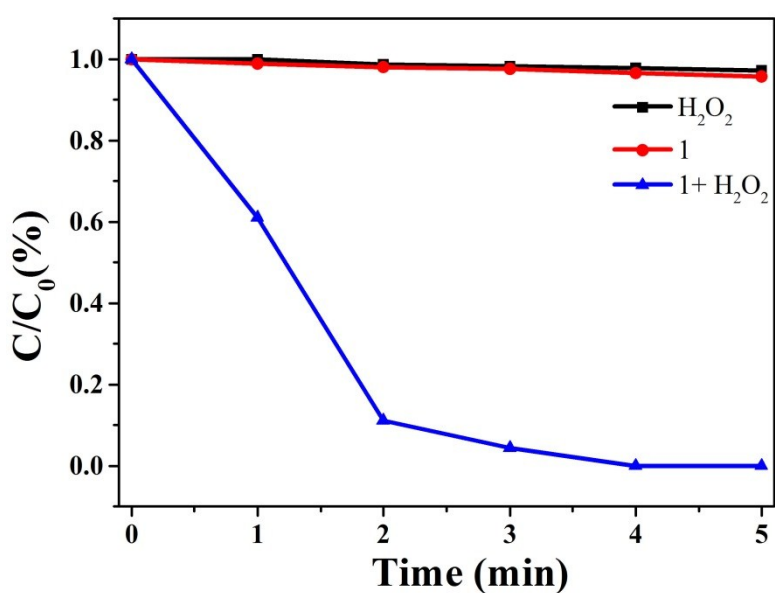


Figure S12. The time dependent UV-Vis spectra of MB over photocatalyst.

References

- [1] O.V. kDolomanov, L.J. Bourhis, R.J. Gildea, J.A.K. Howard, H.J. Puschmann, *Appl. Cryst.* **2009**, 42, 339-341.
- [2] G.M. Sheldrick, *Acta Cryst.* **2008**, A64, 112-122
- [3] G.M. Sheldrick, *Acta Cryst.* 2015, C71, 3-8.